Comparative Investigation of System-Level Optimized Power Conversion System Architectures to Reduce LCOE for Large-Scale PV-Plus-Storage Farms

Zheng An, Rajendra Prasad Kandula, Deepak Divan
School of Electrical and Computer Engineering
Georgia Institute of Technology
Atlanta, GA 30332, USA
zheng.an@gatech.edu

***Abstract*— PV-plus-storage (PVS) has become a prevalent configuration for newly commissioned large-scale solar projects. However, the optimal power conversion system (PCS) architecture has not been investigated yet. This paper first validates the limited impact of inverter cost on LCOE and then explores a system-level optimized PCS architecture with extended LCOE reduction to proliferate large-scale dispatchable solar energy. Two state-of-the-art architectures including central inverters (CI), traditional 480/600 V string inverters (SI) are compared with newly proposed medium voltage string inverters (MVSI) and multiport DC transformer (MDCT). With verified layouts and single line diagrams (SLDs) of 20 MW PVS plants, the losses and costs breakdown of different architectures are extracted and the PCS-related LCOEs are derived. In this analysis, all electrical bill of materials (EBOS) elements, inverters, battery storage and its associated components, are included, whose losses and costs are obtained from markets, manufacturers, and literature. Besides, the sensitivities of PCS-related LCOEs to Inverter-Loading-Ratio (ILR) are also investigated. The results show that compared with CI and SI with 1.5 kV PV, 4 kV MVSI and 34 kV MDCT present an extended LCOE reduction across all ILR from 1.0 to 3.0, making them economically favorable candidates for PVS farms.**

Keywords*— *PV-plus-storage (PVS), solar-plus-storage, optimal system architecture, levelized cost of energy (LCOE), central inverters, string inverters, medium voltage string inverters, multiport DC transformer, electrical bill of materials (EBOS), inverter-loading-ratio (ILR).

I. INTRODUCTION

PV-plus-storage (PVS) has become a prevalent configuration for newly commissioned large-scale PV farms, thanks to declining PV and battery storage cost, and improved energy dispatchability and grid services with added storage [1-3]. Some optimizations have been conducted to increase energy generation and profitability, including PV array sizing [4], storage sizing [5, 6], and storage operations [7]. However, the optimization of the power conversion system (PCS), which bridges the PV modules, storage, and grid, has not been investigated yet.

There are some limitations in the state-of-the-art technologies, including central and traditional 480/600 V string inverters. They feature either a low-voltage DC or a low voltage AC distribution with underground cables inside solar farms, inducing significant power losses and costs. Furthermore, these approaches require either an additional isolated converter or one more transformer winding to integrate the added battery storage, resulting in extra investment and maintenance effort [8]. To further reduce the LCOE and meet the U.S. Department of Energy's 2030 goal of \$0.02/kWh for utility-scale PV, the balance-of-system (BOS), in addition to the dominant PV modules, plays a critical role in cost reduction [2, 3]. One major component of BOS cost is the electrical BOS (EBOS), including current collection, power conversion, transformer isolation, and breakers, which is primarily driven by the inverter's technology. To reduce the EBOS, PV farm distribution can be adapted from $\leqslant$ 1.5 kV low-voltage DC (LVDC) to 4/13/34 kV MVAC, which can reduce the copper losses in the farm distribution dramatically. Furthermore, MVAC collection can be easily fulfilled by using overhead lines, presenting roughly 5-10 times less cost than underground cables, with tremendously reduced labor. As a result, an extended LCOE reduction at system level could be achieved despite a higher cost in inverters themselves.

In this paper, the limited impact of inverter cost on overall LCOE is firstly proved. Then, state-of-the-art architectures, i.e. central inverters (CI) and traditional 480V/600V string inverters (SI), are compare with newly proposed 4 kV/13 kV medium voltage string inverters (MVSI) [9] and multiport DC transformer (MDCT) [10] to find out a system-level optimized PCS architecture with extended LCOE reduction. The comparison is based on 20 MW PV farms with four architectures and includes all EBOS elements, inverters, battery storage and its associated components. Losses and cost breakdown of all PCS architectures are extracted based on derived farm layout and SLDs. In the end, PCS-related LCOEs of all architectures are calculated with NREL tool and compared. And their sensitivities to ILR are also investigated.

II. LIMITED IMPACT OF INVERTER COST

Although inverter cost has been a key area of focus for many years, a quantitative analysis of its impact on LCOE has not been found in existing literature. Based on NREL ATB data [11] and First Solar's design for 20 MW CI-based PV farms, even a zero inverter cost only yields a 3% LCOE reduction, as shown in TABLE I and II. Therefore, a system view is required to reduce LCOE further to proliferate low-cost solar energy.

This work is sponsored by U.S. DOE under the award DE-EE0008351

TABLE III. OVERNIGHT CAPITAL COST (OCC)

	OCC ($/Wdc)	Benchmark ($)
	Module	0.31
BOS	Inverter	**0.04 → 0**
BOS	EBOS	0.096
BOS	SBOS	0.20
Others	Labor	0.14
Others	Design & Engineering	0.01
Others	Permitting & Interconnection	0.02
Others	Civil	0.02
Others	Supply Chain, Logistics & Misc.	0.03
Others	Taxes	0.04
Others	Overhead & Margin	0.14
	Total	**1.046 → 1.006**

TABLE IV. IMPACT OF ZERO INVERTER COST ON LCOE

Net Capacity Factor (%)	20%
Annual Energy Production (kWh/ kW)	1725
Overnight Capital Cost OCC ($/ kW)	**1046 → 1006**
Fixed O&M ($/ kW-year)	14
Variable O&M ($/ MWh)	0
Capital Recovery Factor (%)	5.2%
LCOE from NREL Tool ($/MWhr)	**39.11 → 37.93**
LCOE ($/kWh)	**0.0391 → 0.0379**

III. POWER CONVERSION SYSTEM ARCHITECTURES

Fig. 1 shows basic elements of PVS farms that impact LCOE. This paper considers the DC system, PCS, MVAC system, and storage. PV modules, structural balance of system (SBOS), and the impacts of financing and other common factors are out of scope. The DC system includes DC underground cables, fuses, combiners, and disconnectors. The key parameter is the voltage level, which is primarily 1/1.5 kV and may reach 2 kV in the future. The PCS interfaces the DC system to the MVAC system by PV inverters and transformers, whose specifications are different in CI/SI/MVSI/MDCT architectures. Comprised of AC overhead lines and protection components, an MVAC system at various voltage levels (4/13/34 kV) connects the PCS to the substation. Lastly, the 20 MW/80 MWh battery

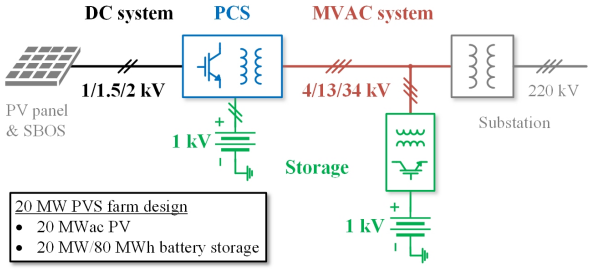

Fig. 1. Basic elements of 20 MW PVS farm.

energy storage system (BESS) contains batteries, associated cables, converters, transformers, and protection elements.

Based on derived single-line diagrams (SLDs) of the 20 MW/80 MWh PVS farm, four different power conversion system architectures, including central inverters (CI), traditional 480/600 V string inverters (SI), 4/13 kV medium-voltage string inverters (MVSI), and 34 kV multiport DC transformer (MDCT), will be compared in terms of their cost, losses and consequent LCOE to find out a system-level optimized architecture with extended LCOE reduction.

A. *Central Inverters (CI)*

Fig. 2 shows the exemplary layouts of 20 MW PV farms with CI architectures, featuring low-voltage DC collection with DC underground cables and centralized 3 MW power conditioning

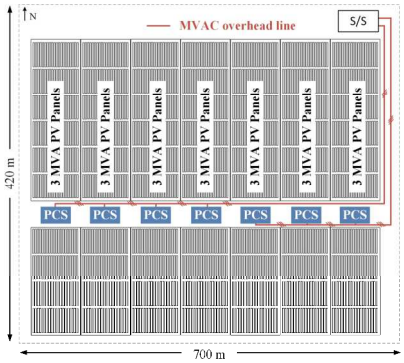

Fig.2. Layout of 20 MW PVS farms with central and string inverters.

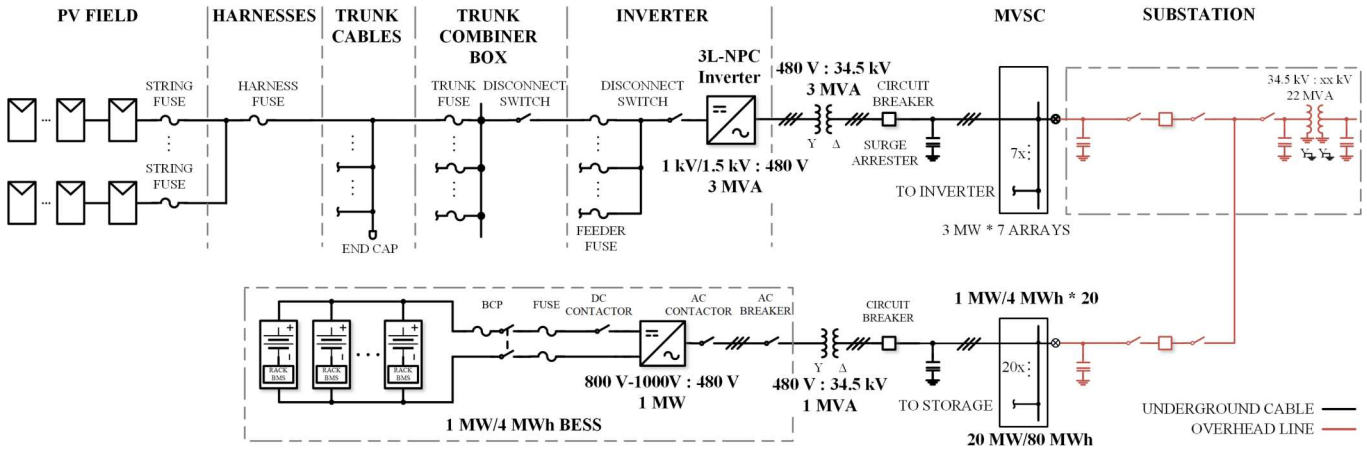

Fig. 3. Single-line digram (SLD) of 20 MW PVS farm with central inverters (CI).

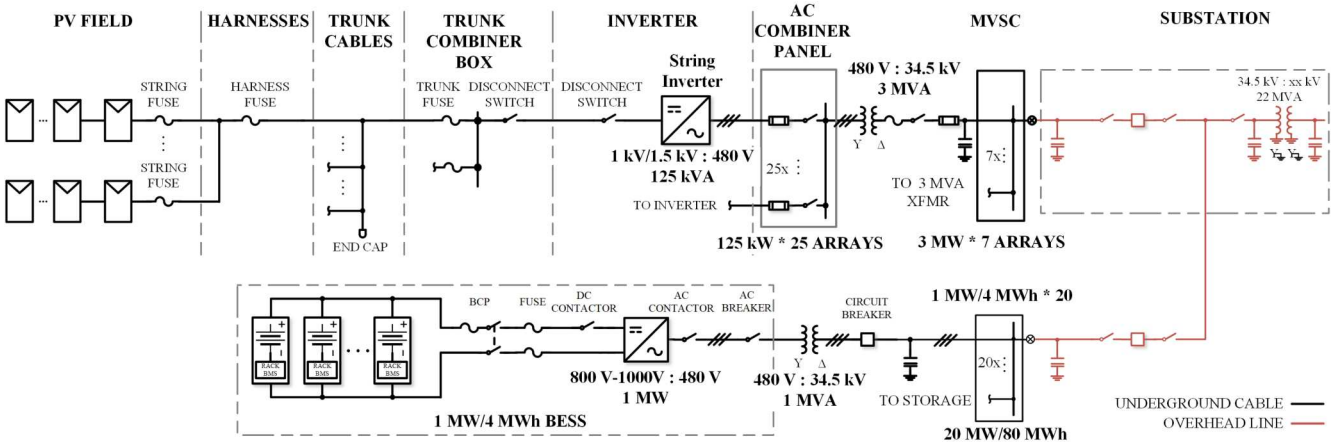

Fig. 4. Single-line digram (SLD) of 20 MW PVS farm with 480/600 V string inverters (SI).

units. The farm layout has been verified by one of solar solution providers.

Fig. 3 presents the SLD of 20 MW PVS farm with CI power electronics building blocks (PEBBs), from PV panels to harness cables, trunk cables, combiner boxes and dc feeders, and PCS, with all protection elements. Twenty of 1 MW/4 MWh storage system turnkey units constitute the 20 MW/80 MWh system [12]. Here ac-coupled centralized BESS is adopted for this approach for its better retrofits.

B. 480/600 V String Inverters (SI)

The 20 MW PVS farm based on traditional 480/600 V low-voltage string inverters shares the same layout shown in Fig. 2.

Fig. 4 presents the SLD of SI architecture, where twenty-five 125 kW string inverter PEBBs are combined right before each 3 MVA centralized transformer. In addition, low-voltage PV power collection is achieved with the use of underground cables. Same as CI approach, ac-coupled BESS configuration is also adopted for this approach.

C. 4/13 kV Medium Voltage String Inverters (MVSI)

Fig. 5 presents the schematic of 300 kVA MVSI, integrating both PV and storage to the MV grid without additional storage converters. Each phase contains 4 modules connected in an input-parallel-output-series way to achieve 3-phase 4 kVac [9].

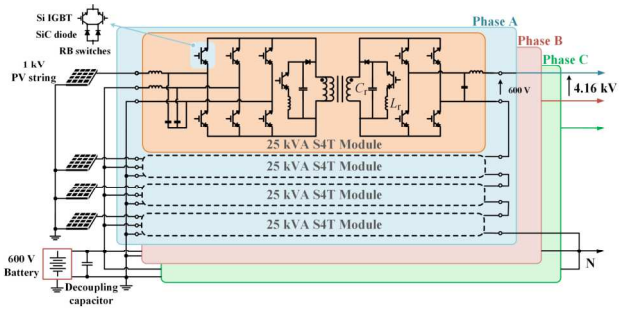

Fig. 5. Schematic of proposed 4 kV/300 kVA MVSI.

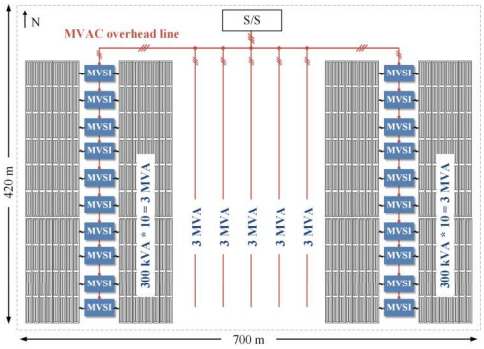

Fig. 6. Layout of 20 MW PVS farm with MVSI and MDCT.

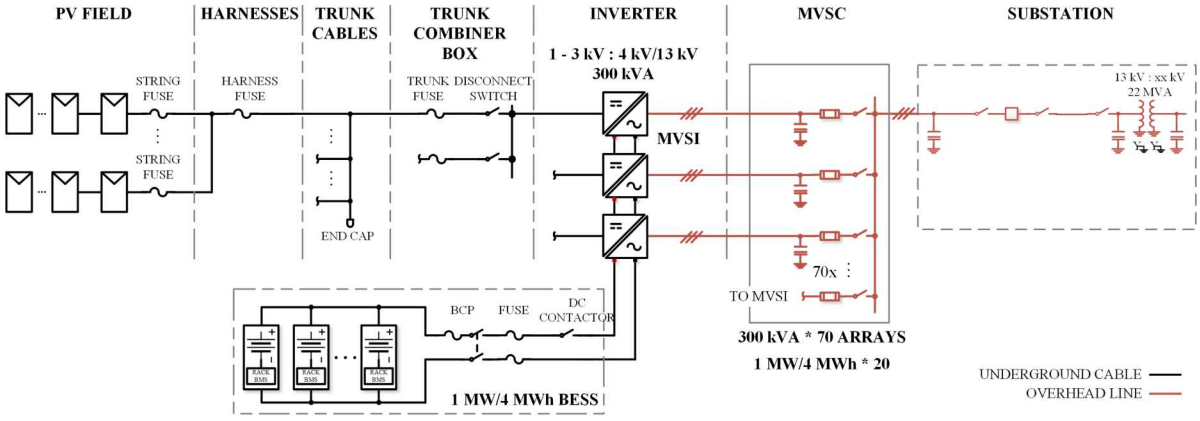

Fig. 7. Single-line digram (SLD) of 20 MW PVS farm with 300 kVA 4/13 kV MVSI PEBBs.

13 kV AC output can be achieved by stacking five modules with 3.3 kV semiconductors.

Fig. 6 shows the layout of 20 MW PVS farm with 300 kVA MVSI PEBBs, where the PEBBs are distributed inside the whole plant. Along with PV panel strings, this "distributed" string inverters layout enables scalable PV farm building blocks. In addition, instead of using underground cables, MVSI enables 4/13 kV MVAC distribution inside PVS farms to fully exploit the advantages of reduced labor with 5-10 times cheaper AC overhead lines (OHL). As a result, the EBOS cost will be significantly reduced.

Fig. 7 illustrates the SLD of 20 MW PVS farm with 300 kVA MVSI PEBBs. Different from those with CI and SI, the tri-port feature of MVSI enables dc-coupled BESS configuration with a plug-and-play connection, resulting in significant cost and losses savings [9, 13]. Every 1 MW/4 MWh storage unit is shared by three 300 kVA MVSI PEBBs in this approach.

D. Multiport DC Transformers (MDCT)

Fig. 8 shows the schematic of 300 kVA MDCT, which integrates PV and storage to three-phase LVAC and then elevates it to 34 kV MVAC via line-frequency transformers. The modular MDCTs are connected in an input-parallel-output-parallel manner to achieve a higher power level [10].

Similar to MVSI approach, MDCT approach shares the same distributed farm layout shown in Fig. 6 but with 34 kV MVAC distribution inside the PV plant. Fig. 9 presents the SLD of 20 MW PVS farm with 34 kV/1 MVA MDCT PEBBs, which also features the dc-coupled BESS configuration. In this approach, each 1 MW/4 MWh storage unit supports one single 1 MVA MDCT PEBB exclusively.

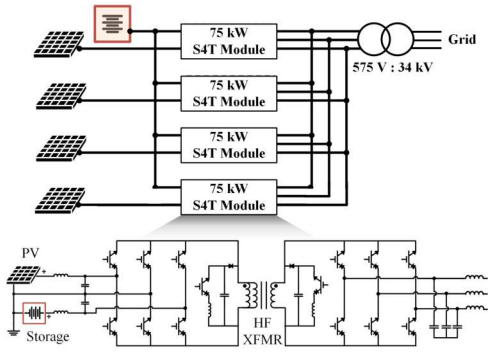

Fig. 8. Schematic of 34 kV multiport DC transformer (MDCT).

IV. Losses and Cost Breakdown

With the detailed SLDs shown above, losses and cost breakdown of four considered architectures have been derived and summarized in Tables III, IV and Fig. 10. In one word, compared with the favored CI with 1.5 kV PV, MVSI and MDCTs present 5% - 15% loss reduction and 3% - 11% cost savings. And the savings expand to 24% in losses and 15% in cost in contrast to traditional 480/600 V SI with 1.5 kV PV. The breakdown of different elements will be explained in detail in following subsections.

A. DC/AC Cables

The specifications of selected cables in four architectures are summarized in TABLE V. The lengths and types of cables in different segments are input from solutions providers, which were selected based on the same current density of cables in corresponding segments of all architectures – a rule of thumb to take the tradeoff of cable losses and cost into account. According to the solution provider, a current density of 100 A/cm^2 was selected for underground buried cables while 170 A/cm^2 for overhead lines. In some segments, different sizes of cables are employed to accommodate the increased flowing current. The cable cost is quoted from cable manufacturers and the losses of harness, trunk cables, and MVAC cables, $P_{harness}$, P_{trunk}, and P_{MVAC}, are calculated with (1):

$$P_{cable} = I_{cable}^2 \cdot R_{cable} \cdot L_{cable} \quad (1)$$

where I_{cable} is the flowing current in different segments of cables, R_{cable} is the unit resistance of different sizes of cables in Ω / m, and L_{cable} is the cable length.

In general, the cable cost and losses decrease with increased voltage levels on both DC and AC sides. In MVSI and MDCT architectures, DC cable savings come from significantly reduced lengths of trunk and feeder cables. On the AC side, the moderate increase in cable length is completely offset by using

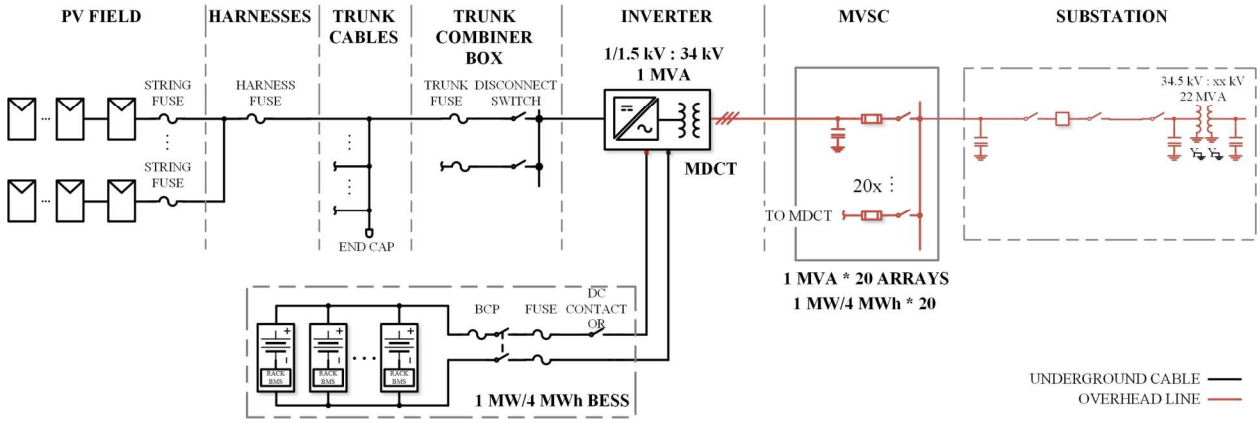

Fig. 9. Single-line digram (SLD) of 20 MW PVS farm with 34 kV MDCTs.

TABLE III. COST COMPARISON IN 20 MW PVS FARMS

(Mil. USD)	CI @ 1 kV DC	CI @ 1.5 kV DC	SI @ 1 kV DC	SI @ 1.5 kV DC	4 kV MVSI @ 1 kV DC	13 kV MVSI @ 1 kV DC	34 kV MDCT @ 1 kV DC	34 kV MDCT @ 2 kV DC
DC	1.22	0.90	1.20	0.83	0.50	0.50	0.50	0.24
Conv Sys.	2.06	1.78	2.38	2.38	3.92	14.10	3.04	3.28
AC	0.14	0.14	0.22	0.22	0.15	0.05	0.02	0.02
Protection	0.30	0.30	0.30	0.30	0.50	0.70	0.20	0.20
∑ PV PCS	3.72	3.12	4.10	3.73	5.07	15.35	3.76	3.74
Storage	13.28	13.28	13.28	13.28	10.80	10.80	10.80	10.80
Total	17.00	16.40	17.38	17.01	15.87	26.15	14.56	14.54

TABLE IV. COMPARISON OF POWER LOSSES AND DELIVERED ENERGY IN 20 MW PVS FARMS

(%)	CI @ 1 kV DC	CI @ 1.5 kV DC	SI @ 1 kV DC	SI @ 1.5 kV DC	4 kV MVSI @ 1 kV DC	13 kV MVSI @ 1 kV DC	34 kV MDCT @ 1 kV DC	34 kV MDCT @ 2 kV DC
DC	0.80	0.50	1.90	1.30	0.10	0.10	0.10	0.03
Conv Sys.	2.49	2.49	2.49	2.49	2.50	2.50	3.09	3.09
AC	0.10	0.10	0.10	0.10	0.90	0.30	0.10	0.10
Storage	4.80	4.73	5.05	4.91	3.93	3.78	3.88	3.86
∑ Loss	8.19	7.82	9.54	8.80	7.43	6.68	7.17	7.08

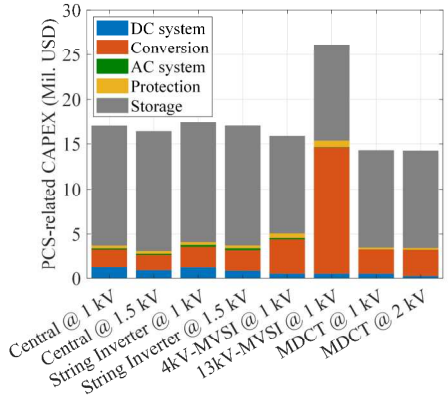

(a)

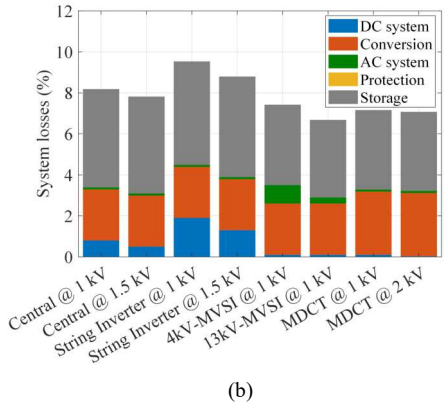

(b)

Fig. 10. Cost and losses comparison of 20 MW PVS farms with CI/SI/MVSI/MDCT architectures.

cheaper MVAC overhead lines than underground cables counterparts.

B. Power Conversion System (Inverters and Transformers)

The PCS includes PV inverters and 34 kV 60 Hz transformers, which are required in CI/SI/MDCT architectures but not in 4 kV/13 kV MVSI.

With the same price benchmarks at component-level from markets and a large manufacturing service company, the bill of materials (BOM) costs of all inverters are estimated and summarized in TABLE VI, where similar component pricing was assumed to make cost comparisons meaningful.

The losses and cost of 34 kV 60 Hz 3-phase transformers are given by a transformer manufacturer, i.e. 0.5% losses and $19/kVA for 3 MVA transformers for PV inverters and 0.6%

TABLE V. SPECIFICATIONS OF CABLES IN FOUR ARCHITECTURES

	1.5 kV CI	1.5 kV SI	4 kV MVSI	13 kV MVSI	34 kV MDCT
Harness	10 AWG Copper (Cu) - 67200 meter (m)	10 AWG Cu -67200 m	10 AWG Cu - 176400 m	10 AWG Cu - 176400 m	10 AWG Cu - 176400 m
Trunk cables	4/0 AWG Aluminum (Al) – 73920 m; 250 MCM Al – 49280 m	250 MCM Al – 123200 m	300 MCM Al – 14000 m	300 MCM Al – 14000 m	300 MCM Al – 14000 m
DC combiner	500 MCM Al – 3640 m	--	--	--	--
Feeder	250/500 MCM Al – 3500/1400 m	1 AWG Al – 10500 m, 1/0 AWG Al – 7000 m	--	--	--
AC combiner	--	1000 MCM Al – 3000 m	--	--	--
MVAC	1/0, 3/0, 4/0 AWG Al – 1200, 1650, 750 m.	1/0, 3/0, 4/0 AWG Al – 1200, 1650, 750 m.	250, 500, 1000 MCM Al – 630, 630, 8400 m	1 AWG, 3/0 AWG, 300, 1000 MCM Al – 630, 630, 1200, 2400 m	5 AWG, 2 AWG, 1/0 AWG, 400 MCM Al – 630, 630, 1200, 2400 m

TABLE VI. BOM COST OF PV INVERTERS IN FOUR ARCHITECTURES

	CI	SI	4 kV MVSI	13 kV MVSI	34 kV MDCT
PV inverters	$81/kVA for 1.5 kV PV; $70/kVA for 1 kV	$100/kVA for 1/1.5 kV PV	$196/kVA for 1 kV PV	$705/kVA for 1 kV PV	$121/kVA for 2 kV PV; $110/kVA for 1 kV
34kV/60 Hz transformers	$19/kVA for 3 MVA units	$19/kVA for 3 MVA units	--	--	$29/kVA for 1 MVA units

losses and $29/kVA for 1 MVA transformers for MDCT and BESS converters. The PCS loss, P_{PCS}, includes those in inverters and transformers (if appropriate).

The cost increases in MVSI mainly comes from the integrated high-frequency transformer and the increased number of semiconductor devices owing to reverse-blocking (RB) switches used in current-source converters. The large increase in the cost of 13 kV MVSI is dominated by the scarcity of 3.3 kV SiC RB devices. Their losses are obtained from the manufacturer's datasheets and test results in literature [14, 15].

C. BESS

According to the latest BloombergNEF report in [16], $135/kWh is used to calculate the 80 MWh battery BOM cost. For the ac-coupled centralized BESS configuration in CI and SI, a 10% increase in DC cable cost is assumed due to the interconnections among battery cells and a 60% increase in AC cables due to substation connection. And $70/kVA is estimated for the 1 MVA storage converter and $29/kVA for the 34 kV 60 Hz transformers.

The roundtrip storage losses, considering 90% charge/discharging efficiency of batteries (95%*95%), are calculate with (2). And they are only applied to the clipped energy delivered to the grid $P_{clipped}$, which is otherwise wasted without added storage. As a result, extra power P_{BESS} captured by paired BESS is delivered to grid. In MVSI and MDCT approaches, 1% losses reduction is achieved by direct power transfer from PV to storage in the converters, without going through external cables and 60 Hz transformers.

$$P_{BESS} = \eta_{charge} \cdot \eta_{discharge} \cdot P_{clipped} = 90\% \cdot P_{clipped} \quad (2)$$

D. Protection

The protection includes fuses, disconnects, circuit breakers, surge arresters, and converter-associated elements. The increased protection cost in MVSI comes from the components against lightning strikes due to the absence of 60 Hz transformers. The reduced cost in MDCT benefits from the elimination of converter-associated components thanks to the cascaded 60 Hz transformers downstream of each MDCT.

V. LCOE EVALUATION AND COMPARISON

To derive LCOE values, the delivered energy to grid in GWh/year at inverter-loading-ratio (ILR) of 2.0 are calculated for all four PCS architectures based on the losses and cost derived above. Next, their LCOEs at ILR = 2.0 are evaluated and compared. At last, the sensitivities of their LCOEs to ILR from 1.0 to 3.0 are investigated.

A. Delivered Energy in GWh/year

In this analysis, normalized PV power generation profile during one day is modelled as a bell-shape curve with (3), where P_{PV} is the generated electric power by solar cell, *ILR* is the inverter-loading-ratio, and σ is geographical dependent [17]. And the clipped energy $P_{clipped}$ is equal to the enclosed area by PV generation profile and 1.0 p.u. normalized PV power line, as shown in Fig. 11. This part of power will be captured by paired BESS to increase the energy revenue of the PV plants.

$$P_{pv} = ILR \cdot e^{-\frac{(t-t_0)^2}{2\sigma^2}} \quad (3)$$

Fig. 12 shows the power flow diagram from PV panels to the grid for the 20 MW/80 MWh PVS farms with all four PCS architectures, including losses in all different segments discussed above. And their delivered energy to the grid in GWh/year are calculated with (4) - (6).

$$P_{grid} = P_{pv} - \sum P_{cable} - P_{PCS} - P_{clipped} + P_{BESS} \quad (4)$$

$$\sum P_{cable} = P_{harness} + P_{trunk} + P_{MVAC} \quad (5)$$

$$W_{grid} = P_{grid} \cdot 20MW \cdot 365days / year \quad (6)$$

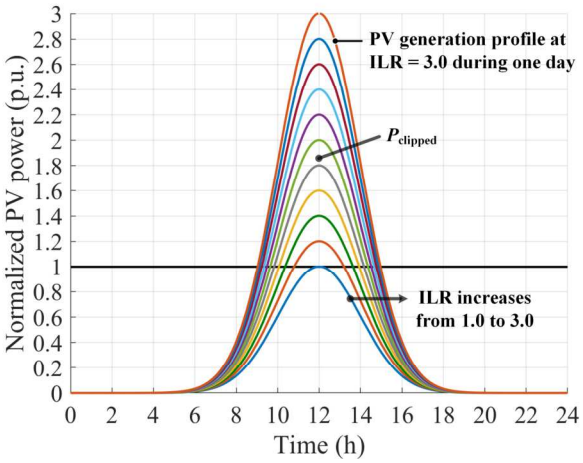

Fig. 11. PV generation profile during one day with different ILRs.

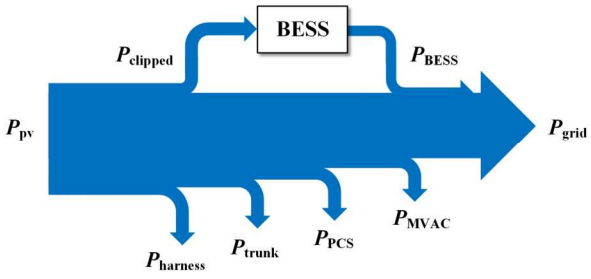

Fig. 12. Power flow diagram of 20 MW/80 MWh PVS farms.

B. LCOE Comparison and Sensitivitiy Analysis

The delivered energy and required costs at ILR of 2.0 are shown in Fig. 12. Compared with the state-of-the-art CI with 1.5 kV PV, the 4 kV MVSI and 34 kV MDCT deliver more energy with less cost, suggesting a decreased LCOE.

Fig. 13 presents the PCS-related LCOE calculated with the NREL tool [11], where the 4 kV MVSI and 34 kV MDCT show reduced PCS-related LCOE across ILR from 1.0 to 3.0 when compared to both the state-of-the-art CI and SI. At ILR = 2.0, a 4% LCOE reduction is achieved by the 4 kV MVSI with 1 kV PV and an even more lucrative 14% reduction by 34 kV MDCT with 2 kV PV in contrast to the CI with 1.5 kV PV. The LCOE reduction in the MVSI approach will expand with elevated PV voltage to 1.5 kV. As a result, these extended LCOE reduction makes them favorable candidates for large-scale PVS farms.

It should be noted that a high LCOE in the 13 kV MVSI is dominated by the extremely expensive 3.3 kV SiC RB devices, even though this approach delivers the most energy. As HV SiC device costs decrease, the cost of the 13 kV MVSI is expected to drop tremendously, leading to superior LCOE when compared to its 4 kV counterpart and at least comparable, if not better, performance when compared to the 34 kV MDCT. Furthermore, a 34 kV MVSI can be developed without increased complexity once 6.5 kV SiC RB devices are economically available, featuring further reduced LCOE and system footprint in contrast to the 34 kV MDCT.

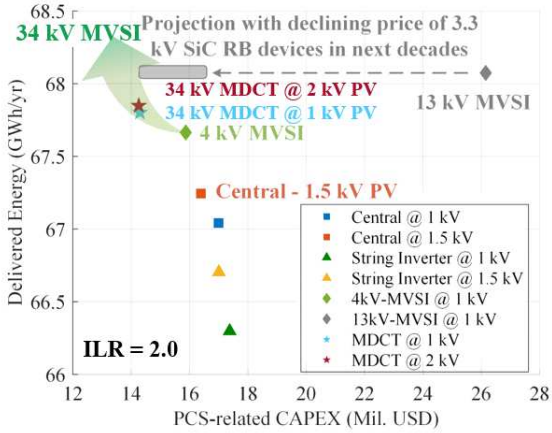

Fig. 13. Schematic of 34 kV multiport DC transformer (MDCT).

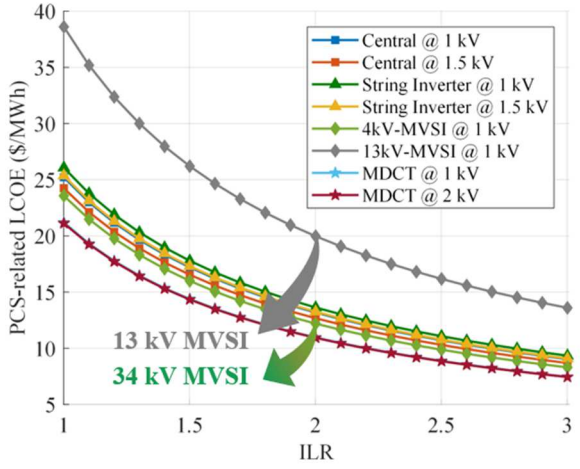

Fig. 14. Schematic of 34 kV multiport DC transformer (MDCT).

VI. Conclusion

This paper validates the limited impact of inverter cost on LCOE and instead investigates system-level optimized PCS architectures to reduce LCOE of large-scale dispatchable solar energy, where the state-of-the-art architectures, i.e. central inverters and traditional 480/600 V string inverters, are compared with recently proposed 4/13 kV MVSI, and 34 kV MDCT. Based on detailed layouts and SLDs of 20 MW PVS farms with four PCS architectures, losses and cost breakdown are derived and compared considering all EBOS elements, inverters, and BESS-related components.

Next, the consequent PCS-related LCOEs are calculated with the NREL tool and their sensitivities to ILR are also investigated. Compared with the state-of-the-art CI with 1.5 kV, MVSI and MDCT present up to 15% loss reduction and a maximum 11% cost savings. And the savings expand to 24% in losses and 15% in cost in contrast to traditional 480/600 V SI with 1.5 kV PV.

In the end, the 4 kV MVSI and MDCTs are validated to present extended LCOE reductions across all ILR from 1.0 to 3.0. At ILR of 2.0, 4 kV MVSI shows a 4% reduction and 34 kV MDCT presents an even more attractive 14% reduction in PCS-related LCOE, making them preferred candidates for large-scale PVS farms. As HV SiC device costs decrease, 13/34 kV MVSI can be developed without added complexity and present reduced system footprint and at least comparable LCOE reduction in comparison with 34 kV MDCT.

Acknowledgment

The authors would like to thank Department of Energy and Center for Distributed Energy at Georgia Tech for their support of this research. In addition, the authors would also like to thank Mahesh, Morjaria from First Solar, Andrew Ingram from Southern Company, for providing their insights and expertise on this analysis. This paper does not reflect any viewpoints of U.S. Department of Energy.

References

[1] A. Perea, C. Smith, M. Davis, X. Sun, S. Rumery, A. Holm, et al., "Us solar market insight executive summary - 2019 year in review," Solar Energy Industries Association SEIA and GTM Research, 2020

[2] P. L. Denholm, R. M. Margolis, and J. D. Eichman, "Evaluating the technical and economic performance of pv plus storage power plants," National Renewable Energy Lab.(NREL), Golden, CO (United States), Tech. Rep., 2017.

[3] R. Fu, T. W. Remo, and R. M. Margolis, "2018 us utility-scale photovoltaics-plus- energy storage system costs benchmark," NREL, Golden, CO (United States), Tech. Rep., 2018.

[4] J. D. Mondol, Y. G. Yohanis, and B. Norton, "Optimal sizing of array and inverter for grid-connected photovoltaic systems," Sol. Energy, vol. 80, no. 12, pp. 1517–1539, 2006.

[5] Y. Ru, J. Kleissl, and S. Martinez, "Storage size determination for grid-connected photovoltaic systems," IEEE Trans. Sustain. Energy, vol. 4, no. 1, pp. 68–81, 2013.

[6] S. A. P. Kani, P. Wild, and T. K. Saha, "Improving Predictability of Renewable Generation through Optimal Battery Sizing," IEEE Trans. Sustain. Energy, vol. 11, no. 1, pp. 37–47, 2020.

[7] Y. Yang, Q. Ye, L. J. Tung, M. Greenleaf, and H. Li, "Integrated Size and Energy Management Design of Battery Storage to Enhance Grid Integration of Large-Scale PV Power Plants," IEEE Transactions on Industrial Electronics, vol. 65, no. 1, pp. 394–402, 2018.

[8] S. Kouro, J. I. Leon, D. Vinnikov, and L. G. Franquelo, "Grid-connected photovoltaic systems: An overview of recent research and emerging pv converter technology," IEEE Industrial Electronics Magazine, vol. 9, no. 1, pp. 47–61, 2015.

[9] Z. An, X. Han, L. Zheng, R. Prasad Kandula, K. Kandasamy, and D. Divan, "Modular isolated soft-switching medium voltage string inverter for large-scale pv farm," in *2020 IEEE Applied Power Electronics Conference and Exposition (APEC)*, 2020

[10] M. Mauger, R. Prasad Kandula, and D. Divan, "A Multiport DC Transformer to Enable Flexible DC as a service," in *2021 IEEE Energy Conversion Congress and Exposition (ECCE)*, 2021, *in press*.

[11] ATB tool, NREL. [Online]. Available: https://atb.nrel.gov/electricity/2018/equations-variables.html

[12] ST1370KWH-1000 datasheet, Sungrow, 2019. [Online]. Available: https://www.sungrowpower.com/sites/default/files/ST1370KWH-1000_datasheet_0.pdf

[13] H. Chen and D. Divan, "Soft-switching solid-state transformer (s4t)," *IEEE Transactions on Power Electronics*, vol. 33, no. 4, pp. 2933–2947, 2018.

[14] HEMK datasheet, Power Electronics, 2020. [Online]. Available: https://www.power-electronics.com/wp-content/uploads/Descargas/Ingles/Leaflets/Solar/Leaflet_HEMK.pdf

[15] L. Zheng, R. P. Kandula, and D. Divan, "Soft-Switching Solid-State Transformer (S4T) with Reduced Conduction Loss," IEEE Transactions on Power Electronics, vol. 8993, no. c, pp. 1–1, 2020

[16] BloombergNEF, "How PV-Plus-Storage Will Compete With Gas Generation in the U.S," 2020.

[17] El-Sharkawi, Mohamed A. *Electric energy: an introduction*. CRC press, 2015.